

Type-to-Track: Retrieve Any Object via Prompt-based Tracking

Pha Nguyen¹, Kha Gia Quach², Kris Kitani³, Khoa Luu¹

¹ CVIU Lab, University of Arkansas ² PDActive Inc. ³ Robotics Institute, Carnegie Mellon University
¹{panguyen, khoaluu}@uark.edu ²kquach@ieee.org ³kkitani@andrew.cmu.edu

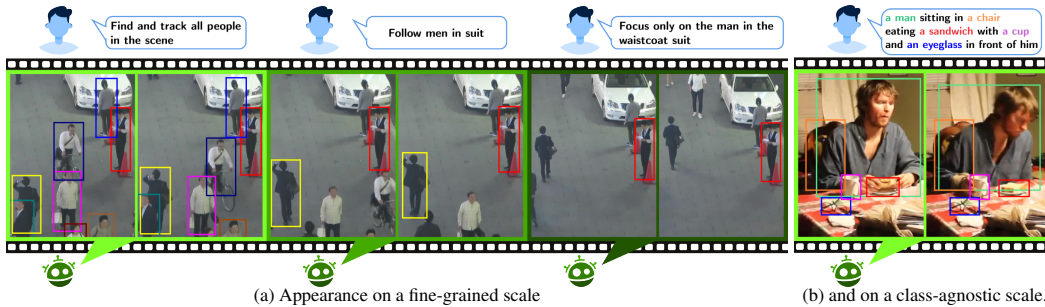


Figure 1: An example of the responsive *Type-to-Track*. The user provides a video sequence and a prompting request. During tracking, the system is able to discriminate appearance attributes to track the target subjects accordingly and iteratively responds to the user’s tracking request. Each box color represents a unique identity.

Abstract

One of the recent trends in vision problems is to use natural language captions to describe the objects of interest. This approach can overcome some limitations of traditional methods that rely on bounding boxes or category annotations. This paper introduces a novel paradigm for Multiple Object Tracking called *Type-to-Track*, which allows users to track objects in videos by typing natural language descriptions. We present a new dataset for that Grounded Multiple Object Tracking task, called *GroOT*, that contains videos with various types of objects and their corresponding textual captions describing their appearance and action in detail. Additionally, we introduce two new evaluation protocols and formulate evaluation metrics specifically for this task. We develop a new efficient method that models a transformer-based eMbed-ENcoDE-extRact framework (*MENDER*) using the third-order tensor decomposition. The experiments in five scenarios show that our *MENDER* approach outperforms another two-stage design in terms of accuracy and efficiency, up to 14.7% accuracy and 4× speed faster.

1 Introduction

Tracking the movement of objects in videos is a challenging task that has received significant attention in recent years. Various methods have been proposed to tackle this problem, including deep learning techniques. However, despite these advances, there is still room for improvement in intuitiveness and responsiveness. One potential way to improve object tracking in videos is to incorporate user input into the tracking process. Traditional Visual Object Tracking (VOT) methods typically require users to manually select objects in the video by bounding boxes or trained object detectors. Thus, in this paper, we introduce a new paradigm, called *Type-to-Track*, to this task that combines responsive typing input to guide the tracking of objects in videos. It allows for more intuitive and conversational

Table 1: Comparison of current datasets. # denotes the number of the corresponding item. **Bold** numbers are the best number in each sub-block, while **highlighted** numbers are the best across all sub-blocks.

Datasets	Task	NLP	#Videos	#Frames	#Tracks	#AnnBoxes	#Words	#Settings
OTB100 [3]	SOT	✗	100	59K	100	59K	-	-
VOT-2017 [4]	SOT	✗	60	21K	60	21K	-	-
GOT-10k [5]	SOT	✗	10K	1.5M	10K	1.5M	-	-
TrackingNet [6]	SOT	✗	30K	14.43M	30K	14.43M	-	-
MOT17 [7]	MOT	✗	42	33.7K	4K	0.9M	-	-
MOT20 [8]	MOT	✗	8	13.41K	3.83K	2.1M	-	-
BDD100K [9]	MOT	✗	2K	318K	130.6K	3.3M	-	-
LaSOT [1]	SOT	✓	1.4K	3.52M	1.4K	3.52M	9.8K	1
TNL2K [2]	SOT	✓	2K	1.24M	2K	1.24M	10.8K	1
GroOT (Ours)	MOT	✓	1,535	2.26M	12K	1M	67.9K	5

tracking, as users can simply type in the name or description of the object they wish to track, as illustrated in Fig. 1. Our intuitive and user-friendly *Type-to-Track* approach has numerous potential applications, such as surveillance and object retrieval in videos.

We present a new Grounded Multiple Object tracking *GroOT* dataset that is more advanced than existing tracking datasets [1, 2]. *GroOT* contains videos with various types of multiple objects and detailed textual descriptions. It is $7\times$ larger and more diverse than existing datasets, and it can construct many different evaluation settings. In addition to three easy-to-construct experimental settings, we propose two new settings for prompt-based visual tracking. It brings the total number of settings to five, which will be presented in Section 5. These new experimental settings challenge existing designs and highlight the potential for further advancements in our proposed research topic.

In summary, this work addresses the use of natural language to guide and assist the Multiple Object Tracking (MOT) tasks with the following contributions. First, a novel paradigm named *Type-to-Track* is proposed, which involves responsive and conversational typing to track any objects in videos. Second, a new *GroOT* dataset is introduced. It contains videos with various types of objects and their corresponding textual descriptions of 67.9K words describing both appearance and action. Next, two new evaluation protocols that are tracking by *retrieval prompts* and *caption prompts*, and two class-agnostic tracking metrics are formulated for this problem. Finally, a new transformer-based eMbed-ENcoDE-extRact framework (*MENDER*) is introduced with third-order tensor decomposition as the first efficient approach for this task. Our contributions in this paper include a novel paradigm, a rich-semantic dataset, an efficient methodology, and challenging benchmarking protocols with new evaluation metrics. These contributions will be advantageous for the field of Grounded MOT by providing a valuable foundation for the development of future algorithms.

2 Related Work

2.1 Visual Object Tracking Datasets and Benchmarks

Datasets. To develop and train VOT models for the computer vision task of tracking objects in videos, various datasets have been created and widely used. Some of the most popular datasets for VOT are OTB [10, 3], VOT [4], GOT [5], MOT challenges [7, 8] and BDD100K [9]. Visual object tracking has two sub-tasks: Single Object Tracking (SOT) and Multiple Object Tracking (MOT). Table 1 shows that there is a wide variety of object tracking datasets in both types available, each with its own strengths and weaknesses. Existing datasets with NLP [1, 2] only support the SOT task, while our *GroOT* dataset supports MOT with approximately $7\times$ larger in description size.

Benchmarks. Current benchmarks for tracking can be broadly classified into two main categories: *Tracking by Bounding Box* and *Tracking by Natural Language*, depending on the type of initialization. Previous benchmarks [11, 10, 3, 4, 12, 13, 13, 14] were limited to test videos before the emergence of deep trackers. The first publicly available benchmarks for visual tracking were OTB-2013 [10] and OTB-2015 [3], consisting of 50 and 100 video sequences, respectively. GOT-10k [5] is a benchmark featuring 10K videos classified into 563 classes and 87 motions. TrackingNet [6], a subset of the object detection benchmark YT-BB [15], includes 31K sequences. Furthermore, there are long-term tracking benchmarks such as OxUvA [16] and LaSOT [1]. OxUvA spans 14 hours

Table 2: Comparison of key features of tracking methods. **Cls-agn.** is for class-agnostic, while **Feat.** is for the approach of feature fusion and **Stages** indicates the number of stages in the model design incorporating NLP into the tracking task. **NLP** indicates how text is utilized for the tracker: *assist* (w/ box) or can *initialize* (w/o box) the process.

Approach	Task	NLP	Cls-agn.	Feat.	Stages
GTI [17]	SOT	assist	✗	concat	single
TransVLT [18]	SOT	assist	✗	attn	single
Tfm [19]	MOT	-	✗	-	-
MDETR+Tfm	MOT	init	✓	attn	two
MENDER	MOT	init	✓	3D-attn	single

Table 3: Statistics for *GroOT* train, val and benchmarking sets.

		#Videos	#Frames	#Tracks	#AnnBoxes	#Words
MOT17**	Train	21	15,948	1,638*	336,891*	3,792
	Val	-	-	-	-	-
	Test	21	17,757	2,355*	564,228*	5,757
	Total	42	33,705	3,993*	901,119*	9,549
TAO**	Train	500	764,526	2,645	54,639	19,222
	Val	993	39,149	5,481	113,112	39,149
	Test	914	2,221,846	7,972	164,650	-
	Total	2,407	4,447,038	16,089	332,401	58,371
GroOT**	cap.	1,535	2,258,897	12,119	1,068,870	67,920
	retr.	993	1,460,666	8,623	-	13,935

* Statistics from the official [site](#) including objects other than human.

** [Creative Commons Attribution-NonCommercial-ShareAlike 3.0 License](#)

of video in 337 videos, comprising 366 object tracks. On the other hand, LaSOT [1] is a language-assisted dataset consisting of 1,4K sequences with 9.8K words in their captions. In addition to these benchmarks, TNL2K [2] includes 2K video sequences for natural language-based tracking and focuses on expressing the attributes. LaSOT [1] and TNL2K [2] support one benchmarking setting with their provided prompts, while our *GroOT* dataset supports five settings.

2.2 Grounded Object Tracking

Grounded Vision-Language involves the model to accurately map language concepts onto visual observations by understanding both vision content and natural language. For instance, visual grounding [20] seeks to identify the location of nouns or short phrases (such as a black hat or a bluebird) within an image. Grounded captioning [21, 22, 23] can generate text descriptions and align predicted words with object regions in an image. Visual dialog [24] enables meaningful dialogues with humans about visual content using natural, conversational language. Some visual dialog systems may incorporate referring expression recognition [25] to resolve expressions in questions or answers.

Grounded Single Object Tracking is limited to tracking a single object with box-initialized and language-assisted methods. The GTI [17] framework decomposes the tracking by language task into three sub-tasks: Grounding, Tracking, and Integration, and generates tubelet predictions frame-by-frame. AdaSwitcher [2] module identifies tracking failure and switches to visual grounding for better tracking. [26] introduce a unified system using attention memory and cross-attention modules with learnable semantic prototypes. Another transformer-based approach [18] is presented including a cross-modal fusion module, task-specific heads, and a proxy token-guided fusion module.

2.3 Discussion

Most existing datasets and benchmarks for object tracking are limited in their coverage and diversity of language and visual concepts. Additionally, the prompts in the existing Grounded SOT benchmarks do not contain variations in covering many objects in a single prompt, which limits the application of existing trackers in practical scenarios. To address this, we present a new dataset and benchmarking metrics to support the emerging trend of the Grounded MOT, where the goal is to align language descriptions with fine-grained regions or objects in videos.

As shown in Table 2, most of the recent methods for the Grounded SOT task are not class-agnostic, meaning they require prior knowledge of the object. GTI [17] and TransVLT [18] need to input the initial bounding box, while Trackformer [19] need the pre-defined category. The operation used in [17] to fuse visual and textual features is *concatenation* which can only support prompts describing a single object. A Grounded MOT can be constructed by integrating a grounded object detector, i.e. MDETR [27], and an object tracker, i.e. Trackformer [19]. However, this approach is low-efficient because the visual features have to be extracted multiple time. In contrast, our proposed MOT approach *MENDER* formulates third-order *attention* to adaptively focus on many targets, and it is an efficient *single-stage* and *class-agnostic* framework. The scope of *class-agnostic* in our approach is constructing a large vocabulary of concepts via a visual-textual corpus, following [28, 29, 30].



Figure 2: Example sequences and annotations in our dataset.

Figure 3: Some words in our language description.

3 Dataset Overview

3.1 Data Collection and Annotation

Existing object tracking datasets are typically designed for specific types of video scenes [32, 33, 34, 35, 36, 37]. To cover a diverse range of scenes, *GroOT* was created using official videos and bounding box annotations from the MOT17 [7] and TAO [31]. The MOT17 dataset comprises 42 sequences with diverse environmental conditions such as crowded scenes, varying viewpoints, and camera motion. The TAO dataset is composed of videos from seven different datasets, such as the ArgoVerse [38] and BDD [9] datasets containing outdoor driving scenes, while LaSOT [1] and YFCC100M [39] datasets include in-the-wild internet videos. Additionally, the AVA [40], Charades [41], and HACS [42] datasets include videos depicting human-human and human-object interactions. By combining these datasets, *GroOT* covers multiple types of scenes and encompasses a wide range of 833 objects. This diversity allows for a wide range of object classes with captions to be included in the dataset, making it an invaluable resource for training and evaluating visual grounding algorithms.

We release our textual description annotations in COCO format [43]. Specifically, a new key ‘captions’ which is a list of strings is attached to each ‘annotations’ item in the official annotation. In the MOT17 subset, we attempt to maintain two types of caption for well-visible objects: one describes the *appearance* and the other describes the *action*. For example, the caption for a well-visible person might be [‘a man wearing a gray shirt’, ‘person walking on the street’] as shown in Fig. 2a. However, 10% of tracklets only have one caption type, and 3% do not have any captions due to their low visibility. In the TAO subset, objects other than humans have one caption describing their appearance, for instance, [‘a red and black scooter’]. Objects that are human have the same two types of captions as the MOT17 subset. An example is shown in Fig. 2b. These captions are consistently annotated throughout the tracklets. Fig. 3 is the word-cloud visualization of our text annotations.

3.2 Type-to-Track Benchmarking Protocols

Let \mathbf{V} be a video sample lasts t frames, where $\mathbf{V} = \{\mathbf{I}_t \mid t < |\mathbf{V}|\}$ and \mathbf{I}_t be the image sample at a particular time step t . We define a request prompt \mathbf{P} that describes the objects of interest, and \mathbf{T}_t is the set of tracklets of interest up to time step t . The *Type-to-Track* paradigm requires a tracker network $\mathcal{T}(\mathbf{I}_t, \mathbf{T}_{t-1}, \mathbf{P})$ that efficiently take into account \mathbf{I}_t , \mathbf{T}_{t-1} , and \mathbf{P} to produce $\mathbf{T}_t = \mathcal{T}(\mathbf{I}_t, \mathbf{T}_{t-1}, \mathbf{P})$. To advance the task of multiple object retrieval, another benchmarking set is created in addition to the *GroOT* dataset. While training and testing sets follow a *One-to-One* scenario, where each caption describes a single tracklet, the new retrieval set contains prompts that follow a *One-to-Many* scenario, where a short prompt describes multiple objects. This scenario highlights the need for diverse methods to improve the task of multiple object retrieval. The retrieval set is provided with a subset of

tracklets in the TAO validation set and three custom *retrieval prompts* that change throughout the tracking process in a video $\{\mathbf{P}_{t_1=0}, \mathbf{P}_{t_2}, \mathbf{P}_{t_3}\}$, as depicted in Fig. 1(a). The *retrieval prompts* are generated through a semi-automatic process that involves: (i) selecting the most commonly occurring category in the video, and (ii) cascadingly filtering to the object that appears for the longest duration. In contrast, the *caption prompts* are created by joining tracklet captions in the scene and keeping it consistent throughout the tracking period. We name these two evaluation scenarios as *tracklet captions* **cap.** and *object retrieval* **retr.** With three more easy-to-construct scenarios, five scenarios in total will be studied for the experiments in Section 5. Table 3 presents the statistics of the two settings, and the data portions are highlighted in the corresponding colors.

3.3 Class-agnostic Evaluation Metrics

As indicated in [44], long-tailed classification is a very challenging task in imbalanced and large-scale datasets such as TAO. This is because it is difficult to distinguish between similar fine-grained classes, such as bus and van, due to the class hierarchy. Additionally, it is even more challenging to treat every class independently. The traditional method of evaluating tracking performance leads to inadequate benchmarking and undesired tracking results. In our *Type-to-Track* paradigm, the main task is not to classify objects to their correct categories but to retrieve and track the object of interest. Therefore, to alleviate the negative effect, we reformulate the original single-category metrics of MOTA [45] and IDF1 [46] into class-agnostic metrics:

$$\text{CA-MOTA} = 1 - \frac{\sum_t \sum_{cls} (\text{FN}_t + \text{FP}_t + \text{IDS}_t)}{\sum_t \sum_{cls} \text{GT}_t}, \quad \text{CA-IDF1} = \frac{\sum_{cls} (2 \times \text{IDTP})}{\sum_{cls} (2 \times \text{IDTP} + \text{IDFP} + \text{IDFN})} \quad (1)$$

where *cls* is the class entry that is accumulated to compute FN, FP, IDS, GT, IDTP, IDFP, and IDFN.

4 Methodology

4.1 Problem Formulation

Given the image \mathbf{I}_t and the request prompt \mathbf{P} describing the objects of interest, which can adaptively change between $\{\mathbf{P}_{t_1}, \mathbf{P}_{t_2}, \mathbf{P}_{t_3}\}$ in the **retr.** setting, and K is the prompt’s length $|\mathbf{P}| = K$, let $\text{enc}(\cdot)$ and $\text{emb}(\cdot)$ be the visual encoder and the word embedding model to extract features of image tokens and prompt tokens, respectively. The resulting outputs, $\text{enc}(\mathbf{I}_t) \in \mathbb{R}^{M \times D}$ and $\text{emb}(\mathbf{P}) \in \mathbb{R}^{K \times D}$, where D is the length of feature dimensions. A list of region-prompt associations \mathbf{C}_t , which contains objects’ bounding boxes and their confident scores, can be produced by Eqn. (2):

$$\mathbf{C}_t = \text{dec}_{\gamma} \left(\text{enc}(\mathbf{I}_t) \bar{\times} \text{emb}(\mathbf{P})^{\top}, \text{enc}(\mathbf{I}_t) \right) = \left\{ \mathbf{c}_i = (c_x, c_y, c_w, c_h, c_{conf})_i \mid i < M \right\}_t \quad (2)$$

where $(\bar{\times})$ is an operation representing the region-prompt correlation, that will be elaborated in the next section, $\text{dec}_{\gamma}(\cdot, \cdot)$ is an object decoder taking the similarity and the image features to decode to object locations, thresholded by a scoring parameter γ (i.e. $c_{conf} \geq \gamma$). For simplicity, the cardinality of the set of objects $|\mathbf{C}_t| = M$, implying each image token produces one region-text correlation.

We define $\mathbf{T}_t = \left\{ \mathbf{tr}_j = (tr_x, tr_y, tr_w, tr_h, tr_{conf}, tr_{id})_j \mid j < N \right\}_t$ produced by the tracker \mathcal{T} , where $N = |\mathbf{T}_t|$ is the cardinality of current tracklets. i, j, k , and t are consistently denoted as indexers for objects, tracklets, prompt tokens, and time steps for the rest of the paper.

Remark 1 Third-order Tensor Modeling. Since the *Type-to-Track* paradigm requires three input components $\mathbf{I}_t, \mathbf{T}_{t-1}$, and \mathbf{P} , an *auto-regressive single-stage end-to-end framework* can be formulated via *third-order tensor modeling*.

To achieve this objective, a combination of initialization, object decoding, visual encoding, feature extraction, word embedding, and aggregation can be formulated as in Eqn. (3):

$$\mathbf{T}_t = \begin{cases} \text{initialize}(\mathbf{C}_t) & t = 0 \\ \text{dec}_{\gamma} \left(\mathbf{1}_{D \times D \times D} \times_1 \text{enc}(\mathbf{I}_t) \times_2 \text{ext}(\mathbf{T}_{t-1}) \times_3 \text{emb}(\mathbf{P}), \text{enc}(\mathbf{I}_t) \right) & \forall t > 0 \end{cases} \quad (3)$$

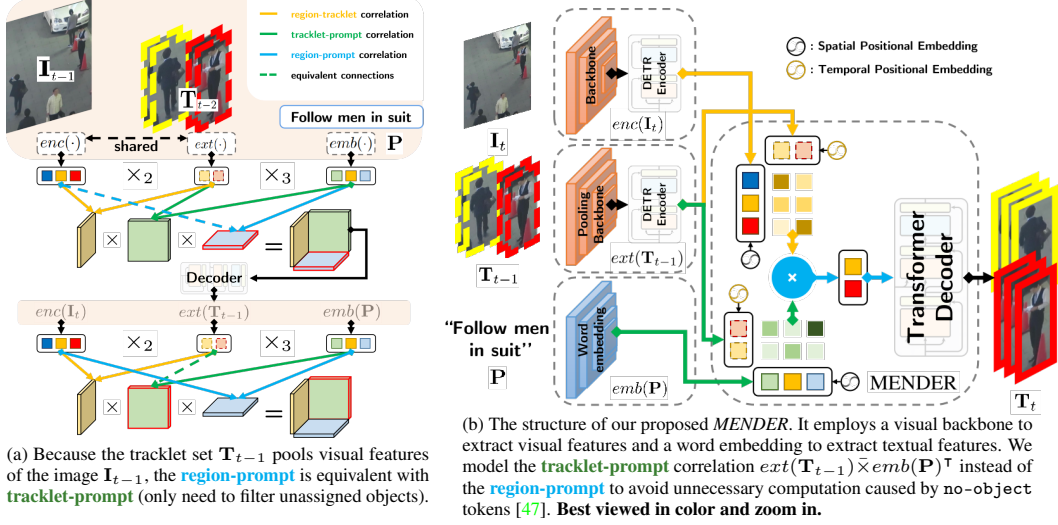


Figure 4: The *auto-regressive* manner takes advantage of the equivalent components. Simplifying the correlation in (a) turns the solution to *MENDER* in (b), and reduces complexity to $\mathcal{O}(n^2)$ where n denotes the size of tokens.

where $ext(\cdot)$ denotes the visual feature extractor of the set of tracklets, $ext(\mathbf{T}_{t-1}) \in \mathbb{R}^{N \times D}$, $\mathbf{1}_{D \times D \times D}$ is an all-ones tensor has size $D \times D \times D$, (\times_n) is the n -mode product of the third-order tensor to aggregate many types of token, and $initialize(\cdot)$ is the function to ascendingly assign unique identities to tracklets for the first time those tracklets appear.

Let $T \in \mathbb{R}^{M \times N \times K}$ be the resulting tensor $T = \mathbf{1}_{D \times D \times D} \times_1 enc(\mathbf{I}_t) \times_2 ext(\mathbf{T}_{t-1}) \times_3 emb(\mathbf{P})$. The objective function can be expressed as the log softmax of the positive region-tracklet-prompt triplet over all possible triplets, defined in Eqn. (4):

$$\theta_{enc, ext, emb}^* = \arg \max_{\theta_{enc, ext, emb}} \left(\log \left(\frac{\exp(T_{ijk})}{\sum_l^K \sum_n^N \sum_m^M \exp(T_{lnm})} \right) \right) \quad (4)$$

where θ denotes the network's parameters, the combination of the i^{th} image token, the j^{th} tracklet, and the k^{th} prompt token is the correlated triplet.

In the next subsection, we elaborate our model design for the tracking function $\mathcal{T}(\mathbf{I}_t, \mathbf{T}_{t-1}, \mathbf{P})$, named *MENDER*, as defined in Eqn. (3), and loss functions for the problem objective in Eqn. (4).

4.2 MENDER for Multiple Object Tracking by Prompts

The correlation in Eqn. (3) has the cubic time and space complexity $\mathcal{O}(n^3)$, which can be intractable as the input length grows and hinder the model scalability.

Remark 2 Correlation Simplification. Since both $enc(\cdot)$ and $ext(\cdot)$ are visual encoders, the **region-prompt** correlation can be equivalent to the **tracklet-prompt** correlation. Therefore, the **region-tracklet-prompt** correlation tensor T can be simplified to lower the computation footprint.

To design that goal, the extractor and encoder share network weights for computational efficiency:

$$ext(\mathbf{T}_{t-1})_j = ext(\{\mathbf{tr}_j\}_{t-1}) = \{enc(\mathbf{I}_{t-1})_i : \mathbf{c}_i \mapsto \mathbf{tr}_j\}, \text{ therefore } ((T_{:j})_{t-1} = (T_{i::})_t) : \mathbf{c}_i \mapsto \mathbf{tr}_j \quad (5)$$

where $T_{:j}$ and $T_{i::}$ are lateral and horizontal slices. In layman's terms, the **region-prompt** correlation at the time step $t-1$ is equivalent to the **tracklet-prompt** correlation at the time step t , as visualized in Fig. 4(a). Therefore, one practically needs to model the **region-tracklet** and **tracklet-prompt** correlations which reduces time and space complexity from $\mathcal{O}(n^3)$ to $\mathcal{O}(n^2)$, significantly lowering computation footprint. We alternatively rewrite the decoding step in Eqn. (3) as:

$$\mathbf{T}_t = dec_{\gamma} \left(\left(enc(\mathbf{I}_t) \bar{\times} ext(\mathbf{T}_{t-1})^\top \right) \times \left(ext(\mathbf{T}_{t-1}) \bar{\times} emb(\mathbf{P})^\top \right), enc(\mathbf{I}_t) \right) \quad \forall t > 0 \quad (6)$$

Correlation Representations. In our approach, the correlation operation ($\bar{\times}$) is modelled by the *multi-head cross-attention* mechanism [48], as depicted in Fig. 4(b). The attention matrix can be computed as:

$$\sigma(\mathbf{X})\bar{\times}\sigma(\mathbf{Y}) = \mathcal{A}_{\mathbf{X}|\mathbf{Y}} = \text{softmax}\left(\frac{(\sigma(\mathbf{X}) \times W_Q^{\mathbf{X}}) \times (\sigma(\mathbf{Y}) \times W_K^{\mathbf{Y}})^{\top}}{\sqrt{D}}\right) \quad (7)$$

where \mathbf{X} and \mathbf{Y} tokens are one of these types: region, tracklet, prompt. $\sigma(\cdot)$ is one of the $enc(\cdot)$, $emb(\cdot)$, $ext(\cdot)$ as the corresponding operation to \mathbf{X} or \mathbf{Y} . Superscript W_Q , W_K , and W_V are the projection matrices corresponding to \mathbf{X} or \mathbf{Y} as in the attention mechanism.

Then, the attention weight from the image \mathbf{I}_t to the prompt \mathbf{P} are computed by the matrix multiplication for $\mathcal{A}_{\mathbf{I}|\mathbf{T}}$ and $\mathcal{A}_{\mathbf{T}|\mathbf{P}}$ to aggregate the information from two matrices as in Eqn. (6). The result is the matrix $\mathcal{A}_{\mathbf{I}|\mathbf{T} \times \mathbf{T}|\mathbf{P}} = \mathcal{A}_{\mathbf{I}|\mathbf{T}} \times \mathcal{A}_{\mathbf{T}|\mathbf{P}}$ that shows the correlation between each input or output. Then, the resulting attention matrix $\mathcal{A}_{\mathbf{I}|\mathbf{T} \times \mathbf{T}|\mathbf{P}}$ is used to produce the object representations at time t :

$$\mathbf{Z}_t = \mathcal{A}_{\mathbf{I}|\mathbf{T} \times \mathbf{T}|\mathbf{P}} \times (\text{emb}(\mathbf{P}) \times W_V^{\mathbf{P}}) + \mathcal{A}_{\mathbf{I}|\mathbf{T}} \times (\text{ext}(\mathbf{T}_{t-1}) \times W_V^{\mathbf{T}}) \quad (8)$$

Object Decoder $dec(\cdot)$ utilizes context-aware features \mathbf{Z}_t that are capable of preserving identity information while adapting to changes in position. The tracklet set \mathbf{T}_t is defined in the *auto-regressive* manner to adjust to the movements of the object being tracked as in Eqn. (6). For decoding the final output at any frame, the decoder transforms the object representation by a 3-layer FFN to predict bounding boxes and confidence scores for frame t :

$$\mathbf{T}_t = \left\{ \mathbf{tr}_j = (tr_x, tr_y, tr_w, tr_h, tr_{conf})_j \right\}_t \stackrel{tr_{conf} \geq \gamma}{=} \text{FFN}\left(\mathbf{Z}_t + \text{enc}(\mathbf{I}_t)\right) \quad (9)$$

where the identification information of tracklets, represented by tr_{id} , is not determined directly by the FFN model. Instead, the tr_{id} value is set when the tracklet is first initialized and maintained till its end, similar to *tracking-by-attention* approaches [19, 49].

4.3 Training Losses

To achieve the training objective function as in Eqn. (4), we formulate the objective function into two loss functions $L_{\mathbf{I}|\mathbf{T}}$ and $L_{\mathbf{T}|\mathbf{P}}$ for correlation training and one loss L_{GIoU} for decoder training:

$$\mathcal{L} = \gamma_{\mathbf{T}|\mathbf{P}} L_{\mathbf{T}|\mathbf{P}} + \gamma_{\mathbf{I}|\mathbf{T}} L_{\mathbf{I}|\mathbf{T}} + \gamma_{GIoU} L_{GIoU} \quad (10)$$

where $\gamma_{\mathbf{T}|\mathbf{P}}$, $\gamma_{\mathbf{I}|\mathbf{T}}$, and γ_{GIoU} are corresponding coefficients, which are set to 0.3 by default.

Alignment Loss $L_{\mathbf{T}|\mathbf{P}}$ is a contrastive loss, which is used to assure the alignment of the ground-truth object feature and caption pairs (\mathbf{T}, \mathbf{P}) which can be obtained in our dataset. There are two alignment losses used, one for all objects normalized by the number of positive prompt tokens and the other for all prompt tokens normalized by the number of positive objects. The total loss can be expressed as:

$$L_{\mathbf{T}|\mathbf{P}} = -\frac{1}{|\mathbf{P}^+|} \sum_k \log\left(\frac{\exp(\text{ext}(\mathbf{T})_j^{\top} \times \text{emb}(\mathbf{P})_k)}{\sum_l \exp(\text{ext}(\mathbf{T})_j^{\top} \times \text{emb}(\mathbf{P})_l)}\right) - \frac{1}{|\mathbf{T}^+|} \sum_j \log\left(\frac{\exp(\text{emb}(\mathbf{P})_k^{\top} \times \text{ext}(\mathbf{T})_j)}{\sum_l \exp(\text{emb}(\mathbf{P})_k^{\top} \times \text{ext}(\mathbf{T})_l)}\right) \quad (11)$$

where \mathbf{P}^+ and \mathbf{T}^+ are the sets of positive prompts and image tokens corresponding to the selected $enc(\mathbf{I})_i$ and $emb(\mathbf{P})_k$, respectively.

Objectness Losses. To model the track’s temporal changes, our network learns from training samples that capture both appearance and motion generated by two adjacent frames:

$$L_{\mathbf{I}|\mathbf{T}} = -\sum_j \log\left(\frac{\exp(\text{ext}(\mathbf{T})_j^{\top} \times \text{enc}(\mathbf{I})_i)}{\sum_l \exp(\text{ext}(\mathbf{T})_j^{\top} \times \text{enc}(\mathbf{I})_l)}\right), \text{ and } L_{GIoU} = \sum_j \ell_{GIoU}(\mathbf{tr}_j, \mathbf{obj}_j) \quad (12)$$

$L_{\mathbf{I}|\mathbf{T}}$ is the log-softmax loss to guide the tokens’ alignment as similar to Eqn. (11). In the L_{GIoU} loss, \mathbf{obj}_j is the ground truth object corresponding to \mathbf{tr}_j . The optimal assignment between \mathbf{tr}_j or \mathbf{obj}_j to the ground truth object is computed efficiently by the Hungarian algorithm, following DETR [47]. ℓ_{GIoU} is the Generalized IoU loss [50].

Table 4: Ablation studies. **sim.** indicates whether the correlation is the *simplified* Eqn. (6) or the Eqn. (3). See 5.1 for the abbreviations. The two first settings get only one word for the request prompt, therefore, tensor T is an un-squeezed matrix, resulting in no difference in **nm.** (X) vs (✓), and **syn.** (X) vs (✓).

P	sim.	CA-MOTA	CA-IDF1	MT	IDs	mAP	FPS
GroOT - MOT17 Subset							
nm.	X/✓	67.00	71.20	1344	1352	0.876	10.3
syn.	X/✓	65.10	71.10	1354	1348	0.874	10.3
def.	X/✓	67.00	72.10	1356	1343	0.876	5.8
	✓	67.30	72.40	1368	1322	0.877	10.3
cap.	X/✓	58.20	53.20	889	1751	0.674	3.4
	✓	59.50	54.80	801	1734	0.688	7.8
GroOT - TAO Subset							
nm.	✓	27.30	37.20	4523	4284	0.212	11.2
syn.	✓	25.70	36.10	4212	5048	0.198	11.2
def.	X/✓	15.20	27.30	3452	6253	0.154	6.2
	✓	16.80	27.70	3547	6118	0.158	10.5
cap.	X/✓	20.30	31.80	3943	5242	0.188	4.3
	✓	20.70	32.00	4103	5192	0.184	8.7
retr.	X/✓	32.40	38.40	630	3238	0.423	7.6
	✓	32.90	39.30	645	3194	0.430	11.5
MOT20							
nm.	X/✓	72.40	67.50	823	2498	0.826	7.6
syn.	X/✓	70.90	65.30	809	2509	0.823	7.6
def.	X/✓	72.90	67.70	823	2489	0.826	4.3
	✓	72.10	67.10	812	2503	0.825	7.6

Table 5: Comparisons to the two-stage baseline design. In each dataset, the from-top-to-bottom scenarios are **syn.**, **def.**, **cap.** and **retr.**. **Best viewed in color.**

Approach	CA-MOTA	CA-IDF1	MT	IDs	mAP	FPS
GroOT - MOT17 Subset						
MDETR + Tfm	62.60	64.70	1319	1382	0.793	2.2
MENDER	65.10	71.10	1354	1348	0.874	10.3
MDETR + Tfm	62.60	64.70	1319	1382	0.793	2.2
MENDER	67.30	72.40	1368	1322	0.877	10.3
MDETR + Tfm	44.80	45.20	693	1945	0.619	2.1
MENDER	59.50	54.80	801	1734	0.688	7.8
GroOT - TAO Subset						
MDETR + Tfm	21.30	33.20	3945	5834	0.184	3.1
MENDER	25.70	36.10	4212	5048	0.198	11.2
MDETR + Tfm	14.60	21.40	2944	6493	0.137	3.1
MENDER	16.80	27.70	3547	6118	0.158	10.5
MDETR + Tfm	15.30	23.60	3132	6354	0.156	3.0
MENDER	20.70	32.00	4103	5192	0.182	8.7
MDETR + Tfm	25.70	26.40	513	3993	0.387	3.1
MENDER	32.90	39.30	645	3194	0.430	11.5
MOT20						
MDETR + Tfm	61.20	60.40	784	2824	0.732	1.9
MENDER	70.90	65.30	809	2509	0.823	7.6
MDETR + Tfm	68.00	66.30	763	2975	0.783	1.9
MENDER	72.10	67.10	812	2503	0.825	7.6

5 Experimental Results

5.1 Implementation Details

Experimental Scenarios. We create three types of prompt: *category name* **nm.**, *category synonyms* **syn.**, *category definition* **def.**. One *tracklet captions* **cap.** scenario is constructed by our detailed annotations and one more *objects retrieval* **retr.** scenario is given in our custom request prompts as described in Subsec. 3.2. The dataset contains 833 classes, each has a name and a corresponding set of synonyms that are different names for the same category, such as [man, woman, human, pedestrian, boy, girl, child] for person. Additionally, each category is described by a *category definition* sentence. This definition makes the model deal with the variations in the text prompts. We join the names, synonyms, definitions, or captions and filter duplicates to construct the prompt. Trained models use the same type as testing.

Datasets and Metrics. RefCOCO+ [51] and Flickr30k [52] serve as pre-trained datasets for acquiring a vocabulary of visual-textual concepts [28]. The $ext(\cdot)$ operation is not involved in this training step. After obtaining a pre-trained model from RefCOCO+ and Flickr30k, we train and evaluate our model for the proposed *Type-to-Track* task on all five scenarios on our *GroOT* dataset and the first-three scenarios for MOT20 [8]. The tracking performance is reported in class-agnostic metrics CA-MOTA and CA-IDF1 as in Eqn. (1) and mAP50 as defined in [31].

Tokens Production. $emb(\cdot)$ utilizes RoBERTa [53] to convert the text input into a sequence of numerical tokens. The tokens are fed into the RoBERTa-base model for text encoding using a 12-layer transformer network with 768 hidden units and 12 self-attention heads per layer. $enc(\cdot)$ is implemented using a ResNet-101 [54] as the backbone to extract visual features from the input image. The output of the ResNet is processed by a Deformable DETR encoder [55] to generate visual tokens. For each dimension, we use sine and cosine functions with different frequencies as positional encodings, similar to [56]. A feature resizer combining a list of (Linear, LayerNorm, Dropout) is used to map to size $D = 512$ for all token producers.

5.2 Ablation Study

Comparisons in Different Scenarios. Table 4 shows comparisons in the performance of different prompt inputs. For MOT17 and MOT20, the *category name* is ‘person’, while *category definition*

is ‘a human being’. Since the prompt by *category definition* is short, it does not differ much from the **nm.** setting. However, the **syn.** setting shuffles between some words, resulting in a slight decrease in CA-MOTA and CA-IDF1. The **cap.** setting results in prompts that contain more diverse and complex vocabulary, and more context-specific information. It is more difficult for the model to accurately localize the objects and identify their identity within the image, as it needs to take into account a wider range of linguistic cues, resulting in a decrease in performance compared to **def.** (59.5% CA-MOTA and 54.8% CA-IDF1 vs 67.3% CA-MOTA and 72.4% CA-IDF1 on MOT17).

For TAO, the **def.** setting has a significant number of variations and many tenuous connections in the scene context, for example, ‘a vehicle carrying many passengers; used for public transport’ for the bus category. Therefore, it results in a decrease in performance (16.8% CA-MOTA and 27.7% CA-IDF1) compared to **cap.** (20.7% CA-MOTA and 32.0% CA-IDF1), because the **cap.** setting is more specific on the object level than category level. The best performant setting is **nm.** (27.3% CA-MOTA and 37.2% CA-IDF1), where names are combined.

Simplified Attention Representations. Table 4 also present the effectiveness of different attention representations of the full tensor T (denoted by \times) and the simplified correlation (denoted by \checkmark). The performance is reported with frame per second (FPS), which is self-measured on one GPU NVIDIA RTX 3060 12GB. Overall, the performance of simplified correlation is witnessed with a superior speed of up to $2\times$ (7.8 FPS vs 3.4 FPS of **cap.** on MOT17 and 11.5 FPS vs 7.6 FPS of **retr.** on TAO) due to fewer computations, resulting in and a slight increase in accuracy due to attention stability, and precision gain.

5.3 Comparisons with a Baseline Design

Due to the new proposed topic, no current work has the same scope or directly solves our problem. Therefore, we compare our proposed *MENDER* against a two-stage baseline tracker in Table 5. We use current SOTA methods to develop this approach, i.e., MDETR [27] for the grounded detector, while Trackformer [19] for the object tracker. It is worth noting that our *MENDER* relies on direct regression to locate and track the object of interest, without the need for an explicit grounded object detection stage. Table 5 shows our proposed *MENDER* outperforms the baseline on both CA-MOTA and CA-IDF1 metrics in all four settings *category synonyms*, *category definition*, *tracklet captions* and *object retrieval* (25.7% vs. 21.3%, 16.8% vs. 14.6%, 20.7% vs. 15.3% and 32.9% vs. 25.7% CA-MOTA on TAO), while can maintain up to $4\times$ run-time speed (10.3 FPS vs 2.2 FPS). The results indicate that training a single-stage network enhances efficiency and reduces errors by avoiding separate feature extractions for both detection and tracking steps.

6 Conclusions

We have presented a novel problem of *Type-to-Track*, which aims to track objects using natural language descriptions instead of bounding boxes or categories, and a large-scale dataset to advance this task. Our proposed *MENDER* model reduces the computational complexity of third-order correlations by designing an efficient attention method that scales quadratically w.r.t the input sizes. Our experiments on three datasets and five scenarios demonstrate that our model achieves state-of-the-art accuracy and speed for class-agnostic tracking.

Limitations. While our proposed metrics effectively evaluate the proposed *Type-to-Track* problem, they may not be ideal for measuring precision-recall characteristics in retrieval tasks. Additionally, the lack of the question-answering task in data and problem formulation may limit the algorithm to not being able to provide language feedback such as clarification or alternative suggestions. Additional benchmarks incorporating question-answering are excellent research avenues for future work.

Broader Impacts. The *Type-to-Track* problem and the proposed *MENDER* model have the potential to impact various fields, such as surveillance and robotics, where recognizing object interactions is a crucial task. By reformulating the problem with text support, the proposed methodology can improve the intuitiveness and responsiveness of tracking, making it more practical for video input support in large-language models [57] and real-world applications similar to ChatGPT. However, it could bring potential negative impacts related to human trafficking by providing a video retrieval system via text.

References

- [1] Heng Fan, Liting Lin, Fan Yang, Peng Chu, Ge Deng, Sijia Yu, Hexin Bai, Yong Xu, Chunyuan Liao, and Haibin Ling. Lasot: A high-quality benchmark for large-scale single object tracking. In *Proceedings of the IEEE Conference on Computer Vision and Pattern Recognition*, pages 5374–5383, 2019. 2, 3, 4
- [2] Xiao Wang, Xiujun Shu, Zhipeng Zhang, Bo Jiang, Yaowei Wang, Yonghong Tian, and Feng Wu. Towards more flexible and accurate object tracking with natural language: Algorithms and benchmark. In *Proceedings of the IEEE/CVF Conference on Computer Vision and Pattern Recognition (CVPR)*, pages 13763–13773, June 2021. 2, 3, 17
- [3] Yi Wu, Jongwoo Lim, and Ming-Hsuan Yang. Object tracking benchmark. *IEEE Transactions on Pattern Analysis and Machine Intelligence*, 37(9):1834–1848, 2015. 2
- [4] Matej Kristan, Jiri Matas, Aleš Leonardis, Tomas Vojir, Roman Pflugfelder, Gustavo Fernandez, Georg Nebehay, Fatih Porikli, and Luka Čehovin. A novel performance evaluation methodology for single-target trackers. *IEEE Transactions on Pattern Analysis and Machine Intelligence*, 38(11):2137–2155, Nov 2016. 2
- [5] Lianghua Huang, Xin Zhao, and Kaiqi Huang. Got-10k: A large high-diversity benchmark for generic object tracking in the wild. *IEEE Transactions on Pattern Analysis and Machine Intelligence*, 2019. 2
- [6] Matthias Muller, Adel Bibi, Silvio Giancola, Salman Alsubaihi, and Bernard Ghanem. Trackingnet: A large-scale dataset and benchmark for object tracking in the wild. In *Proceedings of the European Conference on Computer Vision (ECCV)*, pages 300–317, 2018. 2
- [7] A. Milan, L. Leal-Taixé, I. Reid, S. Roth, and K. Schindler. MOT16: A benchmark for multi-object tracking. *arXiv:1603.00831 [cs]*, March 2016. arXiv: 1603.00831. 2, 4, 14
- [8] Patrick Dendorfer, Hamid Rezaatofghi, Anton Milan, Javen Shi, Daniel Cremers, Ian Reid, Stefan Roth, Konrad Schindler, and Laura Leal-Taixé. Mot20: A benchmark for multi object tracking in crowded scenes. *arXiv preprint arXiv:2003.09003*, 2020. 2, 8
- [9] Fisher Yu, Haofeng Chen, Xin Wang, Wenqi Xian, Yingying Chen, Fangchen Liu, Vashisht Madhavan, and Trevor Darrell. BDD100K: A diverse driving dataset for heterogeneous multitask learning. In *IEEE/CVF Conference on Computer Vision and Pattern Recognition (CVPR)*, June 2020. 2, 4
- [10] Yi Wu, Jongwoo Lim, and Ming Hsuan Yang. Object tracking benchmark. *IEEE Transactions on Pattern Analysis & Machine Intelligence*, 37(9):1834, 2015. 2
- [11] Pengpeng Liang, Erik Blasch, and Haibin Ling. Encoding color information for visual tracking: Algorithms and benchmark. *IEEE Transactions on Image Processing*, 24(12):5630–5644, 2015. 2
- [12] A Li, M Lin, Y Wu, MH Yang, and S Yan. NUS-PRO: A New Visual Tracking Challenge. *IEEE Transactions on Pattern Analysis and Machine Intelligence*, 38(2):335–349, 2016. 2
- [13] Siyi Li and Dit-Yan Yeung. Visual object tracking for unmanned aerial vehicles: A benchmark and new motion models. In *Proceedings of the AAAI Conference on Artificial Intelligence*, volume 31, 2017. 2
- [14] Hamed Kiani Galoogahi, Ashton Fagg, Chen Huang, Deva Ramanan, and Simon Lucey. Need for speed: A benchmark for higher frame rate object tracking. In *Proceedings of the IEEE International Conference on Computer Vision*, pages 1125–1134, 2017. 2
- [15] Esteban Real, Jonathon Shlens, Stefano Mazzocchi, Xin Pan, and Vincent Vanhoucke. Youtube-boundingboxes: A large high-precision human-annotated data set for object detection in video. In *proceedings of the IEEE Conference on Computer Vision and Pattern Recognition*, pages 5296–5305, 2017. 2
- [16] Jack Valmadre, Luca Bertinetto, Joao F Henriques, Ran Tao, Andrea Vedaldi, Arnold WM Smeulders, Philip HS Torr, and Efstratios Gavves. Long-term tracking in the wild: A benchmark. In *Proceedings of the European Conference on Computer Vision (ECCV)*, pages 670–685, 2018. 2
- [17] Zhengyuan Yang, Tushar Kumar, Tianlang Chen, Jingsong Su, and Jiebo Luo. Grounding-tracking-integration. *IEEE Transactions on Circuits and Systems for Video Technology*, 31(9):3433–3443, 2020. 3
- [18] Haojie Zhao, Xiao Wang, Dong Wang, Huchuan Lu, and Xiang Ruan. Transformer vision-language tracking via proxy token guided cross-modal fusion. *Pattern Recognition Letters*, 2023. 3
- [19] Tim Meinhardt, Alexander Kirillov, Laura Leal-Taixe, and Christoph Feichtenhofer. Trackformer: Multi-object tracking with transformers. In *Proceedings of the IEEE/CVF Conference on Computer Vision and Pattern Recognition*, pages 8844–8854, 2022. 3, 7, 9
- [20] Fenglin Liu, Xian Wu, Shen Ge, Xuancheng Ren, Wei Fan, Xu Sun, and Yuexian Zou. Dimbert: learning vision-language grounded representations with disentangled multimodal-attention. *ACM Transactions on Knowledge Discovery from Data (TKDD)*, 16(1):1–19, 2021. 3

- [21] Wenqiao Zhang, Haochen Shi, Siliang Tang, Jun Xiao, Qiang Yu, and Yueting Zhuang. Consensus graph representation learning for better grounded image captioning. In *Proceedings of the AAAI Conference on Artificial Intelligence*, volume 35, pages 3394–3402, 2021. 3
- [22] Wenhui Jiang, Minwei Zhu, Yuming Fang, Guangming Shi, Xiaowei Zhao, and Yang Liu. Visual cluster grounding for image captioning. *IEEE Transactions on Image Processing*, 31:3920–3934, 2022. 3
- [23] Jialian Wu, Jianfeng Wang, Zhengyuan Yang, Zhe Gan, Zicheng Liu, Junsong Yuan, and Lijuan Wang. Grit: A generative region-to-text transformer for object understanding. *arXiv preprint arXiv:2212.00280*, 2022. 3
- [24] Haonan Yu, Haichao Zhang, and Wei Xu. Interactive grounded language acquisition and generalization in a 2d world. In *International Conference on Learning Representations*, 2018. 3
- [25] Sahar Kazemzadeh, Vicente Ordonez, Mark Matten, and Tamara Berg. Referitgame: Referring to objects in photographs of natural scenes. In *Proceedings of the 2014 conference on empirical methods in natural language processing (EMNLP)*, pages 787–798, 2014. 3
- [26] Yihao Li, Jun Yu, Zhongpeng Cai, and Yuwen Pan. Cross-modal target retrieval for tracking by natural language. In *Proceedings of the IEEE/CVF Conference on Computer Vision and Pattern Recognition*, pages 4931–4940, 2022. 3
- [27] Aishwarya Kamath, Mannat Singh, Yann LeCun, Gabriel Synnaeve, Ishan Misra, and Nicolas Carion. Mdetr-modulated detection for end-to-end multi-modal understanding. In *Proceedings of the IEEE/CVF International Conference on Computer Vision*, pages 1780–1790, 2021. 3, 9, 21
- [28] Alireza Zareian, Kevin Dela Rosa, Derek Hao Hu, and Shih-Fu Chang. Open-vocabulary object detection using captions. In *Proceedings of the IEEE/CVF Conference on Computer Vision and Pattern Recognition*, pages 14393–14402, 2021. 3, 8
- [29] Muhammad Maaz, Hanoona Bangalath Rasheed, Salman Hameed Khan, Fahad Shahbaz Khan, Rao Muhammad Anwer, and Ming-Hsuan Yang. Multi-modal transformers excel at class-agnostic object detection. *arXiv*, 2021. 3
- [30] Tanmay Gupta, Amita Kamath, Aniruddha Kembhavi, and Derek Hoiem. Towards general purpose vision systems: An end-to-end task-agnostic vision-language architecture. In *Proceedings of the IEEE/CVF Conference on Computer Vision and Pattern Recognition*, pages 16399–16409, 2022. 3
- [31] Achal Dave, Tarasha Khurana, Pavel Tokmakov, Cordelia Schmid, and Deva Ramanan. Tao: A large-scale benchmark for tracking any object. In *Computer Vision—ECCV 2020: 16th European Conference, Glasgow, UK, August 23–28, 2020, Proceedings, Part V 16*, pages 436–454. Springer, 2020. 4, 8, 14
- [32] Andreas Geiger, Philip Lenz, Christoph Stiller, and Raquel Urtasun. Vision meets robotics: The kitti dataset. *The International Journal of Robotics Research*, 32(11):1231–1237, 2013. 4
- [33] Jordi Pont-Tuset, Federico Perazzi, Sergi Caelles, Pablo Arbeláez, Alex Sorkine-Hornung, and Luc Van Gool. The 2017 DAVIS Challenge on Video Object Segmentation. *arXiv*, 2017. 4
- [34] Linjie Yang, Yuchen Fan, and Ning Xu. Video instance segmentation. In *ICCV*, 2019. 4
- [35] Ning Xu, Linjie Yang, Yuchen Fan, Dingcheng Yue, Yuchen Liang, Jianchao Yang, and Thomas Huang. YouTube-VOS: A Large-Scale Video Object Segmentation Benchmark. *arXiv*, 2018. 4
- [36] Jiyang Qi, Yan Gao, Yao Hu, Xinggang Wang, Xiaoyu Liu, Xiang Bai, Serge Belongie, Alan Yuille, Philip HS Torr, and Song Bai. Occluded video instance segmentation: A benchmark. *International Journal of Computer Vision*, 130(8):2022–2039, 2022. 4
- [37] Namdar Homayounfar, Justin Liang, Wei-Chiu Ma, and Raquel Urtasun. Videoclick: Video object segmentation with a single click. *arXiv preprint arXiv:2101.06545*, 2021. 4
- [38] Ming-Fang Chang, John Lambert, Patsorn Sangkloy, Jagjeet Singh, Slawomir Bak, Andrew Hartnett, De Wang, Peter Carr, Simon Lucey, Deva Ramanan, et al. Argoverse: 3d tracking and forecasting with rich maps. In *Proceedings of the IEEE/CVF conference on computer vision and pattern recognition*, pages 8748–8757, 2019. 4
- [39] Bart Thomee, David A Shamma, Gerald Friedland, Benjamin Elizalde, Karl Ni, Douglas Poland, Damian Borth, and Li-Jia Li. Yfcc100m: The new data in multimedia research. *Communications of the ACM*, 59(2):64–73, 2016. 4
- [40] Chunhui Gu, Chen Sun, David A Ross, Carl Vondrick, Caroline Pantofaru, Yeqing Li, Sudheendra Vijayanarasimhan, George Toderici, Susanna Ricco, Rahul Sukthankar, et al. Ava: A video dataset of spatio-temporally localized atomic visual actions. In *Proceedings of the IEEE conference on computer vision and pattern recognition*, pages 6047–6056, 2018. 4
- [41] Gunnar A Sigurdsson, Gül Varol, Xiaolong Wang, Ali Farhadi, Ivan Laptev, and Abhinav Gupta. Hollywood in homes: Crowdsourcing data collection for activity understanding. In *Computer Vision—ECCV 2016: 14th European Conference, Amsterdam, The Netherlands, October 11–14, 2016, Proceedings, Part I 14*, pages 510–526. Springer, 2016. 4

- [42] Hang Zhao, Antonio Torralba, Lorenzo Torresani, and Zhicheng Yan. Hacs: Human action clips and segments dataset for recognition and temporal localization. In *Proceedings of the IEEE/CVF International Conference on Computer Vision*, pages 8668–8678, 2019. 4
- [43] Tsung-Yi Lin, Michael Maire, Serge Belongie, James Hays, Pietro Perona, Deva Ramanan, Piotr Dollár, and C Lawrence Zitnick. Microsoft coco: Common objects in context. In *Computer Vision—ECCV 2014: 13th European Conference, Zurich, Switzerland, September 6–12, 2014, Proceedings, Part V 13*, pages 740–755. Springer, 2014. 4
- [44] Siyuan Li, Martin Danelljan, Henghui Ding, Thomas E Huang, and Fisher Yu. Tracking every thing in the wild. In *Computer Vision—ECCV 2022: 17th European Conference, Tel Aviv, Israel, October 23–27, 2022, Proceedings, Part XXII*, pages 498–515. Springer, 2022. 5
- [45] Keni Bernardin and Rainer Stiefelhagen. Evaluating multiple object tracking performance: the clear mot metrics. *EURASIP Journal on Image and Video Processing*, 2008:1–10, 2008. 5
- [46] Ergys Ristani, Francesco Solera, Roger Zou, Rita Cucchiara, and Carlo Tomasi. Performance measures and a data set for multi-target, multi-camera tracking. In *European conference on computer vision*, pages 17–35. Springer, 2016. 5
- [47] Nicolas Carion, Francisco Massa, Gabriel Synnaeve, Nicolas Usunier, Alexander Kirillov, and Sergey Zagoruyko. End-to-end object detection with transformers. In *Computer Vision—ECCV 2020: 16th European Conference, Glasgow, UK, August 23–28, 2020, Proceedings, Part I 16*, pages 213–229. Springer, 2020. 6, 7
- [48] Ashish Vaswani, Noam Shazeer, Niki Parmar, Jakob Uszkoreit, Llion Jones, Aidan N Gomez, Łukasz Kaiser, and Illia Polosukhin. Attention is all you need. *Advances in neural information processing systems*, 30, 2017. 7
- [49] Fangao Zeng, Bin Dong, Yuang Zhang, Tiancai Wang, Xiangyu Zhang, and Yichen Wei. Motr: End-to-end multiple-object tracking with transformer. In *European Conference on Computer Vision (ECCV)*, 2022. 7
- [50] Hamid Rezatofighi, Nathan Tsoi, JunYoung Gwak, Amir Sadeghian, Ian Reid, and Silvio Savarese. Generalized intersection over union. In *The IEEE Conference on Computer Vision and Pattern Recognition (CVPR)*, June 2019. 7
- [51] Licheng Yu, Patrick Poirson, Shan Yang, Alexander C Berg, and Tamara L Berg. Modeling context in referring expressions. In *Computer Vision—ECCV 2016: 14th European Conference, Amsterdam, The Netherlands, October 11–14, 2016, Proceedings, Part II 14*, pages 69–85. Springer, 2016. 8
- [52] Bryan A. Plummer, Liwei Wang, Christopher M. Cervantes, Juan C. Caicedo, Julia Hockenmaier, and Svetlana Lazebnik. Flickr30k entities: Collecting region-to-phrase correspondences for richer image-to-sentence models. *IJCV*, 123(1):74–93, 2017. 8
- [53] Yinhan Liu, Myle Ott, Naman Goyal, Jingfei Du, Mandar Joshi, Danqi Chen, Omer Levy, Mike Lewis, Luke Zettlemoyer, and Veselin Stoyanov. Roberta: A robustly optimized bert pretraining approach. *arXiv preprint arXiv:1907.11692*, 2019. 8, 20
- [54] Kaiming He, Xiangyu Zhang, Shaoqing Ren, and Jian Sun. Deep residual learning for image recognition. In *Proceedings of the IEEE conference on computer vision and pattern recognition*, pages 770–778, 2016. 8
- [55] Xizhou Zhu, Weijie Su, Lewei Lu, Bin Li, Xiaogang Wang, and Jifeng Dai. Deformable {detr}: Deformable transformers for end-to-end object detection. In *International Conference on Learning Representations*, 2021. 8, 20
- [56] Yuqing Wang, Zhaoliang Xu, Xinlong Wang, Chunhua Shen, Baoshan Cheng, Hao Shen, and Huaxia Xia. End-to-end video instance segmentation with transformers. In *Proceedings of the IEEE/CVF conference on computer vision and pattern recognition*, pages 8741–8750, 2021. 8
- [57] OpenAI. Gpt-4 technical report. *arXiv*, 2023. 9
- [58] Boris Sekachev, Nikita Manovich, Maxim Zhiltsov, Andrey Zhavoronkov, Dmitry Kalinin, Ben Hoff, TOsmanov, Dmitry Kruchinin, Artyom Zankevich, DmitriySidnev, Maksim Markelov, Johannes222, Mathis Chenuet, a andre, telenachos, Aleksandr Melnikov, Jijoong Kim, Liron Ilouz, Nikita Glazov, Priya4607, Rush Tehrani, Seungwon Jeong, Vladimir Skubriev, Sebastian Yonekura, vugia truong, zliang7, lizhming, and Tritin Truong. opencv/cvat: v1.1.0, August 2020.
- [59] Antoine Yang, Antoine Miech, Josef Sivic, Ivan Laptev, and Cordelia Schmid. Tubedetr: Spatio-temporal video grounding with transformers. In *Proceedings of the IEEE/CVF Conference on Computer Vision and Pattern Recognition*, pages 16442–16453, 2022. 20
- [60] Jingkuan Song, Ruimin Lang, Xiaosu Zhu, Xing Xu, Lianli Gao, and Heng Tao Shen. 3d self-attention for unsupervised video quantization. In *Proceedings of the 43rd International ACM SIGIR Conference on Research and Development in Information Retrieval*, pages 1061–1070, 2020. 20

- [61] Haoyu Lan, Alzheimer Disease Neuroimaging Initiative, Arthur W Toga, and Farshid Sepehrband. Three-dimensional self-attention conditional gan with spectral normalization for multimodal neuroimaging synthesis. *Magnetic resonance in medicine*, 86(3):1718–1733, 2021. 20
- [62] Yang Liu, Idil Esen Zulfikar, Jonathon Luiten, Achal Dave, Deva Ramanan, Bastian Leibe, Aljoša Ošep, and Laura Leal-Taixé. Opening up open world tracking. In *Proceedings of the IEEE/CVF Conference on Computer Vision and Pattern Recognition*, pages 19045–19055, 2022. 21

Appendix

7 Dataset Taxonomy

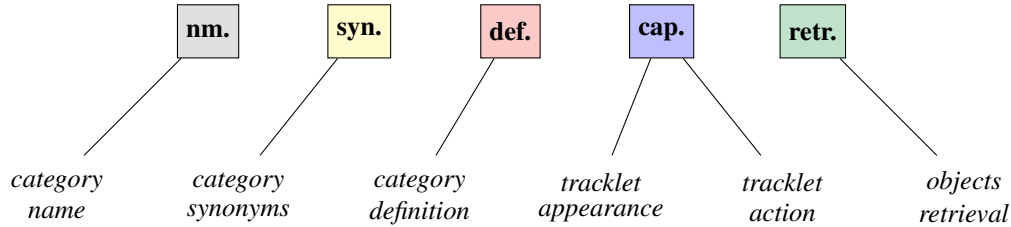


Figure 5: Full list of the types of caption to construct the request prompt for the corresponding settings.

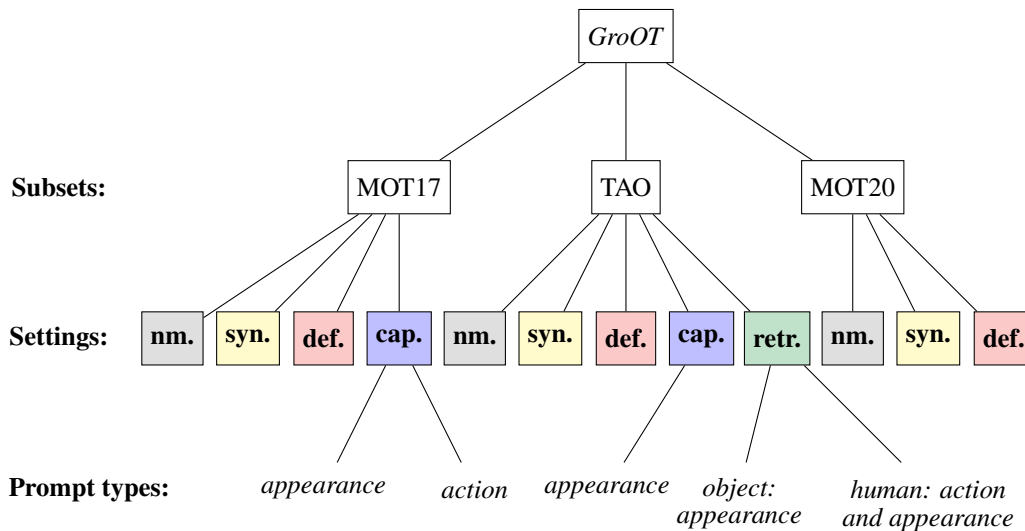


Figure 6: Types of prompt for the construction of our settings for each dataset.

The reason for creating two new evaluation scenarios **cap.** and **retr.** is that they are more specific on the object level than on the category level. This is because defining objects by category synonyms and category name and definition is not sufficient to accurately describe them, and leads to ambiguous results. By focusing on the object level, the benchmarking sets can provide more accurate and meaningful evaluations of multiple object retrieval methods.

We include a comprehensive taxonomy of prompt types used to construct our settings. However, the **retr.** setting on the MOT17 could not be constructed because test annotations for this dataset are not available. To construct this setting, bounding boxes will be filtered to the corresponding **retrieval prompt** when it changes. Section 8 describes how to construct this **retrieval prompt**. The MOT20 dataset requires extensive annotations and has a larger number of low-visible people due to the crowd view. Therefore, its annotations are not ready to be released at the moment.

8 Annotation Process

Instead of collecting new videos, we add annotations to the widely used MOT17 [7] and TAO [31] evaluation sets. These sets contains diverse and relatively long videos with fast-moving objects, camera motion, various object sizes, frequent object occlusions, scale changes, motion blur, and similar objects. Another advantage is that there are typically multiple objects that are present throughout the full sequence, which is desirable for long-term tracking scenarios.

We entrust 10 professional annotators to annotate all frames. All annotations are manually verified.

Then, we post-process the annotations to construct the *retrieval prompts*. Retrieval prompts are short phrases or sentences used to retrieve relevant information from the video. The process of generating these prompts involves two main steps:

1. Select the most commonly occurring category in the video. This is done to ensure that the generated prompts are relevant to the content of the video and that they capture the main objects or scenes in the video. For example, if the video is about a soccer game, the most commonly occurring category might be 'soccer players' or 'soccer ball'.
2. Filter the category selected in the first step to the object that appears for the longest duration. This is likely done to ensure that the generated prompts are specific and focused on a particular object or scene in the video. For example, if the most commonly occurring category in a soccer game video is 'soccer players', the longest appearing player is selected as the focus of the retrieval prompt.

9 Data Format

9.1 categories

```
1 categories [{
2     'frequency': str,
3     'id': int,
4     'synset': str,
5     'image_count': int,
6     'instance_count': int,
7     'name': str
8     'synonyms': [str],
9     'def': str
10 }]
```

The categories field of the annotation structure stores a mapping of category id to the category name, synonyms, and definitions. The categories field is structured as an array of dictionaries. Each dictionary in the array represents a single category.

The keys and values of the dictionary are:

- 'frequency': A string value that indicates the frequency of the category in the dataset.
- 'id': An integer value that represents the unique ID assigned to the category.
- 'synset': A string value that contains a unique identifier for the category.
- 'image_count': An integer value that indicates the number of images in the dataset that belong to the category.
- 'instance_count': An integer value that indicates the number of instances of the category that appear in the dataset.
- 'name': A string value that represents the name of the category.
- 'synonyms': An array of string values that contains synonyms of the category name.
- 'def': A string value that provides a definition of the category.

9.2 annotations

```
1 annotations [{
2     'id': int,
3     'image_id': int,
4     'category_id': int,
5     'scale_category': str,
6     'track_id': int,
7     'video_id': int,
```

```

8     'segmentation': [polygon],
9     'area': float,
10    'bbox': [x, y, width, height],
11    'iscrowd': 0 or 1,
12    'captions': [str]
13  }]

```

An object instance annotation is a record that describes a single instance of an object in an image or video. It is structured as a dictionary that contains a series of key-value pairs, where each key corresponds to a specific field in the annotation. The fields included in the annotation are:

- 'id': An integer value that represents the unique ID assigned to the annotation.
- 'image_id': An integer value that represents the ID of the image that the object instance is part of.
- 'category_id': An integer value that represents the ID of the category to which the object instance belongs.
- 'scale_category': A string value that represents the scale of the object instance with respect to the category.
- 'track_id': An integer value that represents the ID of the track to which the object instance belongs.
- 'video_id': An integer value that represents the ID of the video that the object instance is part of.
- 'segmentation': An array of polygon coordinates that represent the segmentation mask of the object instance.
- 'area': A float value that represents the area of the object instance.
- 'bbox': An array of four values that represent the bounding box coordinates of the object instance.
- 'iscrowd': A binary value (0 or 1) that indicates whether the object instance is a single object or a group of objects.
- 'captions': An array of string values that contains annotated textual descriptions of the object instance. The first caption is implicitly annotated as appearance, while the next one is action.

9.3 images

```

1  images [{
2      'id': int,
3      'frame_index': int,
4      'video_id': int,
5      'file_name': str,
6      'width': int,
7      'height': int,
8      'video': str,
9      'prompt': str
10 }]

```

The images annotations are used to construct request prompts by using the image index at a particular timestamp. To do this, we use the 'images' field in the annotation structure, which contains information about the images in the dataset.

Each image in the dataset is represented as a dictionary object with the following fields:

- 'id': an integer ID for the image
- 'frame_index': an integer value representing the frame index or time stamp index of the image

- ‘video_id’: an integer ID for the video the image belongs to
- ‘file_name’: a string value representing the name of the image file
- ‘width’: an integer value representing the width of the image in pixels
- ‘height’: an integer value representing the height of the image in pixels
- ‘video’: a string value representing the name of the video the image belongs to
- ‘prompt’: a string value representing the request prompt for the video at a particular time stamp which is indexed by ‘frame_index’.

The ‘prompt’ field is the key field used to construct the request prompt, and it is generated based on the information in the annotations for the objects in the image. By using the annotations to generate the prompt, it becomes possible to retrieve specific data about the objects in the image, such as their category, location, and size.

10 Examples

10.1 Data Samples



Figure 7: Samples in TNL2K [2] dataset. The annotations are not meaningful and not discriminative. This dataset also overlooks many moving objects that are present in the video but are not annotated.

In Fig. 7, we present some samples from the TNL2K [2] dataset. This dataset only contains SOT annotations, which are less meaningful than our dataset. For example, the annotations for some objects in the images, such as ‘the batman’, ‘the first person on the left side’, and ‘the animal riding a motor’, can be confusing for both viewers and algorithms. In some cases, the same caption describes two different objects. For instance, in a video game scene, two different opponents are annotated with the same caption ‘the target person the player against with’. Additionally, this dataset overlooks some large moving objects present in the video. Therefore, while the TNL2K dataset provides some useful data, it also has significant limitations in terms of the clarity, discrimination, and consistency of the annotations, and the scope of the annotated objects.

On the other hand, Fig. 8 shows some samples from our *GroOT* dataset, which covers almost all moving objects in the video and provides distinct captions. The dataset includes a variety of object types and provides accurate and comprehensive annotations such as ‘white tissues on a table’, ‘a bottle on the table’, etc. This allows for more effective training and evaluation of Grounded MOT algorithms.

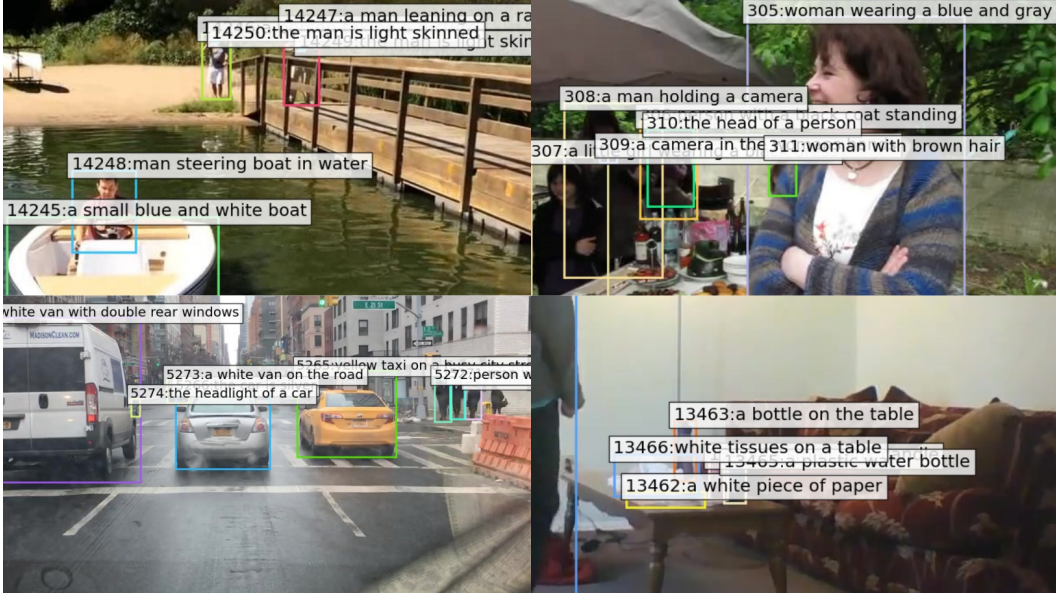


Figure 8: Samples in our *GroOT* dataset cover almost all moving objects with discriminative captions and a variety of object types. Labels are shown in the following format: `track_id:np.random.choice(captions)`.

10.2 Annotations

Table 6: Examples of annotations in the *GroOT* dataset.

MOT17	
‘name’	‘person’
‘synonyms’	[‘baby’, ‘child’, ‘boy’, ‘girl’, ‘man’, ‘woman’, ‘pedestrian’, ‘human’]
‘def’	‘a human being’
‘captions’	[‘man walking on sidewalk’, ‘man wearing a orange shirt’]
TAO	
‘name’	‘backpack’
‘synonyms’	[‘backpack’, ‘knapsack’, ‘packsack’, ‘rucksack’, ‘haversack’]
‘def’	‘a bag carried by a strap on your back or shoulder’
‘captions’	[‘a black colored bag’, ‘the bag is yellow in color’]
‘prompt’	‘woman carrying two bags’

Table 6 provides examples of annotations in the *GroOT* dataset. For instance, the MOT17 subset has annotations for the object class ‘person’ with synonyms including ‘baby’, ‘child’, ‘boy’, ‘girl’, ‘man’, ‘woman’, ‘pedestrian’ and ‘human’. The definition for this class is ‘a human being’ and example captions could include ‘man walking on sidewalk’ or ‘man wearing an orange shirt’. On the other hand, the TAO subset has annotations for the object class ‘backpack’, with synonyms such as ‘knapsack’, ‘packsack’, ‘rucksack’, and ‘haversack’. The definition for this class is ‘a bag carried by a strap on your back or shoulder’ and example captions could include ‘a black colored bag’ or ‘the bag is yellow in color’. In addition to these annotations, the retrieval prompt is included, which provides a textual description of the objects being tracked in a given video sequence, such as ‘woman carrying two bags’.

10.3 Run-time Prompts

Table 7 presents examples of how the annotations described earlier can be used to construct request prompts during runtime. In MOT17 and MOT20 subsets, the only category is ‘person’ with randomly selected synonyms ‘man’ and ‘woman’ and the definition ‘a human being’. The

Table 7: Examples of constructing request prompts in the proposed evaluation settings.

	MOT17	MOT20
nm.	‘person’	‘person’
syn.	[‘man’, ‘woman’]	[‘man’, ‘woman’]
def.	[‘a human being’]	[‘a human being’]
cap.	[‘a man in a suit’, ‘man wearing an orange shirt’, ‘a woman in a black shirt and pink skirt’]	N/A
TAO		
<i>Example 1</i>		
nm.	[‘bus’, ‘bicycle’, ‘person’]	
syn.	[‘autobus’, ‘bicycle’, ‘pedestrian’]	
def.	[‘a vehicle carrying many passengers; used for public transport’, ‘a motor vehicle with two wheels and a strong frame’, ‘a human being’]	
cap.	[‘a black van’, ‘silver framed bicycle’, ‘person wearing black pants’]	
retr.	‘people crossing the street’	
<i>Example 2</i>		
nm.	[‘man’, ‘cup’, ‘chair’, ‘sandwich’, ‘eyeglass’]	
syn.	[‘person’, ‘cup’, ‘chair’, ‘sandwich’, ‘spectacles’]	
def.	[‘a human being’, ‘a small open container usually used for drinking; usually has a handle’, ‘a seat for one person, with a support for the back’, ‘two (or more) slices of bread with a filling between them’, ‘optical instrument consisting of a frame that holds a pair of lenses for correcting defective vision’]	
cap.	[‘a man wearing a gray shirt’, ‘a white cup on the table’, ‘wooden chair in white room’, ‘the sandwich is triangle’, ‘an eyeglasses on the table’]	
retr.	‘a man sitting on a chair eating a sandwich with a cup and an eyeglass in front of him’	

captions for the MOT17 subset include ‘a man in a suit’, ‘man wearing an orange shirt’ and ‘a woman in a black shirt and pink skirt’, while the captions for the MOT20 subset are not annotated.

For TAO subset, the categories in the first example on a driving scene include ‘bus’, ‘bicycle’ and ‘person’ with the synonyms being ‘autobus’, ‘bicycle’ and ‘pedestrian’, respectively. The definitions for these categories are ‘a vehicle carrying many passengers; used for public transport’, ‘a motor vehicle with two wheels and a strong frame’ and ‘a human being’, respectively. The captions include ‘a black van’, ‘silver framed bicycle’, and ‘person wearing black pants’, while the retrieval is ‘people crossing the street’.

Example 2 shows another example of how annotations can be used to construct request prompts. The categories in this example include ‘man’, ‘cup’, ‘chair’, ‘sandwich’ and ‘eyeglass’ with the synonyms being ‘person’, ‘cup’, ‘chair’, ‘sandwich’ and ‘spectacles’, respectively. The definitions for these categories are ‘a human being’, ‘a small open container usually used for drinking; usually has a handle’, ‘a seat for one person, with a support for the back’, ‘two (or more) slices of bread with a filling between them’ and ‘optical instrument consisting of a frame that holds a pair of lenses for correcting defective vision’, respectively. The joint captions include ‘a man wearing a gray shirt’, ‘a white cup on the table’, ‘wooden chair in white room’, ‘the sandwich is triangle’ and ‘an eyeglass on the table’, while the

retrieval prompt is ‘a man sitting on a chair eating a sandwich with a cup and an eyeglass in front of him’.

11 Methodology

11.1 3D Transformers

Third-order Tensor Modeling. Our design of third-order tensor to handle three input components \mathbf{I}_t , \mathbf{T}_{t-1} , and \mathbf{P} influences the design of a novel 3D Transformer. Current temporal visual-text modeling [59, 60, 61] uses two dimensions and computes interactions between video and text features, which are then spanned over the temporal domain. However, our approach is different because it handles three components individually, which allows for more flexibility and a more nuanced understanding of the data. By modeling as the n -mode product of the third-order tensor to aggregate many types of tokens, we have presented a general methodology that can be scaled to multi-modality. The use of the 3D Transformer model, which allows for interactions between these features over time, can improve the performance of multi-modal models by enabling them to consider a wider range of input features and their temporal dependencies. Therefore, our design of third-order tensor modeling has the potential for further research in multi-modality applications.

11.2 Symmetric Alignment Loss

Both the *Alignment Loss* $L_{\mathbf{T}|\mathbf{P}}$ and the *Objectness Loss* $L_{\mathbf{I}|\mathbf{T}}$ are log-softmax loss functions because they both aim to maximize the similarity of the alignments. The *Alignment Loss* has two terms, one for all objects normalized by the number of positive prompt tokens and the other for all prompt tokens normalized by the number of positive objects. In this way, the loss is symmetric and penalizes equally both types of misalignments, especially for *different modalities*.

On the other hand, the *Objectness Loss* only computes from one side and is not necessarily symmetric because there is a *single modality* in this case. It only needs to focus on the quality of the object alignment to the image and does not need to take into account the quality of the image alignment to the object. Consider two objects A and B are equivalent. If we want to maximize the similarity between object A and the correct alignment, we can achieve this by computing the loss on A with B or B with A . The similarity between object A and object B is maximized in both cases.

12 Additional Experimental Results

Pseudo-Algorithm. Alg. 1 is the pseudo-code for our *MENDER* algorithmic design, a Grounded Multiple Object Tracker that performs online multiple object tracking via text initialization. The pseudocode provides a high-level overview of the steps involved in our *MENDER* method.

Prompt Change without Losing Track. If \mathbf{P} changes to a new prompt between $\{\mathbf{P}_{t_1}, \mathbf{P}_{t_2}, \mathbf{P}_{t_3}\}$ that still covers a subset of the objects from the previous prompt, then the **region-prompt** correlation is still partially equivalent to the **tracklet-prompt** correlation. In this case, our *MENDER* can still attend to the correct targets even with the new prompt, because it is trained to maximize the correct pairs which are influenced by the *Alignment Loss* and *Objectness Loss*.

However, if the prompt \mathbf{P} changes completely and no longer covers any of the objects from the previous prompt, then our *MENDER* needs to reinitialize the process by recomputing the **region-prompt**. This means that the algorithm needs to start over with the new **region-prompt** correlation and determine which objects to attend to, as in line 13 to line 14.

Training Process. We follow the same training setting as [55] with a batch size of 4, 40 epochs, and different learning rates for the word embedding model, and the rest of the network, specifically, the learning rates are 0.00005, and 0.0001, respectively. We configure different max numbers for each type of token: 250 for text queries, 500 for image queries, and 500 for tracklet queries. The training takes about 4 days for MOT17 and 7 days for MOT20 and TAO on 4 GPUs NVIDIA A100.

Text Tokenizer. *MENDER* employs RoBERTa Tokenizer [53] to convert textual input into a sequence of text tokens. This is done by dividing the text into a sequence of subword units using a pre-existing vocabulary. Each subword is then mapped to a unique numerical token ID using a lookup table.

Algorithm 1 The inference pipeline of *MENDER*

Input: Video \mathbf{V} , set of tracklets $\mathbf{T} \leftarrow \emptyset$, set of prompts $\{\mathbf{P}_{t_1=0}, \mathbf{P}_{t_2}, \mathbf{P}_{t_3}\}$, $\gamma = 0.7$,
 $\gamma_{reassign} = 0.75, t_{tlr} = 30$

- 1: **for** $t \in \{0, \dots, |\mathbf{V}| - 1\}$ **do**
- 2: **if** $t \in \{t_1, t_2, t_3\}$ **then**
- 3: Select $\mathbf{P} \leftarrow \mathbf{P}_t$
- 4: **end if**
- 5: Draw $\mathbf{I}_t \in \mathbf{V}$
- 6: **if** $\mathbf{T} = \emptyset$ **then**
- 7: **if** $t = 0$ **then**
- 8: $\mathbf{T}_{inactive} \leftarrow \emptyset$
- 9: **else**
- 10: *% This case happens when \mathbf{P} changed to a completely new prompt without covering any old tracklets, returning an empty \mathbf{T} at a timestamp $t \geq 0$ in line 23. Then the reinitialization is performed as in line 13 to line 14.*
- 11: Pass
- 12: **end if**
- 13: $\mathbf{C} \leftarrow \text{dec}_{\gamma}(\text{enc}(\mathbf{I}_t) \bar{\times} \text{emb}(\mathbf{P})^{\top}, \text{enc}(\mathbf{I}_t))$
- 14: $\mathbf{T} \leftarrow \text{initialize}(\mathbf{C}_t)$ *% Obtaining tracklet tr_{id} 's*
- 15: **else**
- 16: $\mathbf{T}_{prev} \leftarrow \mathbf{T} + \mathbf{T}_{inactive}$
- 17: *% If \mathbf{P} does not change or it covers a subset of the previous objects, our MENDER forward has the ability to attend to the correct targets.*
- 18: $\mathbf{T} = \text{dec}_{\gamma}(\left(\text{enc}(\mathbf{I}_t) \bar{\times} \text{ext}(\mathbf{T}_{prev})^{\top} \right) \times \left(\text{ext}(\mathbf{T}_{prev}) \bar{\times} \text{emb}(\mathbf{P})^{\top} \right), \text{enc}(\mathbf{I}_t))$
- 19: *% Obtaining tracklet tr_{id} 's*
- 20: $\text{matched_pairs}, \text{unmatched_lists} \leftarrow \text{cascade_matching}(\mathbf{T}, \mathbf{T}_{prev}, \gamma_{reassign})$
- 21: $\text{m_new}, \text{m_old} \leftarrow \text{matched_pairs}$
- 22: $\text{unm_new}, \text{unm_old} \leftarrow \text{unmatched_lists}$
- 23: $\mathbf{T} \leftarrow \text{update}(\mathbf{T}[\text{m_new}], \mathbf{T}_{prev}[\text{m_old}]) + \text{initialize}(\mathbf{T}[\text{unm_new}])$
- 24: $\mathbf{T}_{inactive} \leftarrow \text{remove_deprecation}(\mathbf{T}_{inactive}, t_{tlr}) + \mathbf{T}_{prev}[\text{unm_old}]$
- 25: **end if**
- 26: **end for**

The tokenizer adds special tokens [CLS] and [SEP] to the beginning and end of the sequence, respectively. To encode the prompt for **def.** and **cap.** settings, the [CLS] token is used to represent each sentence in the prompt list, as in Table 6 and Table 7. For **nm.** and **syn.**, we join the words by ‘. ’ and use the word features, following [27].

12.1 Negative Effects of the Long-tail Challenge on Tracking

The imbalance in the TAO’s distribution has negative effects on the performance of tracking algorithms and the evaluation of tracking metrics. Here are the negative effects of the long-tail problem on large-scale tracking datasets:

Inaccurate Classification. Large-scale tracking datasets like TAO contain numerous rare and semantically similar categories [62]. The classification performance for these categories is inaccurate due to the challenges of imbalanced datasets and distinguishing fine-grained classes. The inaccurate classification results in suboptimal tracking, where objects may be misclassified. This hinders the accurate evaluation of tracking algorithms, as classification is a prerequisite for conducting association and evaluating tracking performance.

Suboptimal Tracking. Current MOT methods and metrics typically associate objects with the same class predictions. In the case of large-scale datasets with inaccurate classification, this association strategy leads to suboptimal tracking. Even if the tracker localizes and tracks the object perfectly, it still receives a low score if the class prediction is wrong. As a result, the performance of trackers in

Table 8: Traditional metrics struggle to evaluate tracking performance in the presence of uneven datasets and misclassified categories, leading to biased and extremely poor results.

P	sim.	MOTA	IDF1	CA-MOTA	CA-IDF1	MT	IDs	mAP	FPS
GroOT - MOT17 Subset									
nm.	X/✓	67.00	71.20	67.00	71.20	1344	1352	0.876	10.3
syn.	X/✓	65.10	71.10	65.10	71.10	1354	1348	0.874	10.3
def.	X	67.00	72.10	67.00	72.10	1356	1343	0.876	5.8
	✓	67.30	72.40	67.30	72.40	1368	1322	0.877	10.3
cap.	X	58.20	53.20	58.20	53.20	889	1751	0.674	3.4
	✓	59.50	54.80	59.50	54.80	801	1734	0.688	7.8
GroOT - TAO Subset									
nm.	✓	3.10	-53.20	27.30	37.20	4523	4284	0.212	11.2
syn.	✓	3.00	-57.10	25.70	36.10	4212	5048	0.198	11.2
def.	X	1.70	-62.10	15.20	27.30	3452	6253	0.154	6.2
	✓	1.70	-62.10	16.80	27.70	3547	6118	0.158	10.5
cap.	X	1.90	-62.00	20.30	31.80	3943	5242	0.188	4.3
	✓	1.90	-60.20	20.70	32.00	4103	5192	0.184	8.7
retr.	X	4.50	-45.60	32.40	38.40	630	3238	0.423	7.6
	✓	4.50	-45.60	32.90	39.30	645	3194	0.430	11.5
MOT20									
nm.	X/✓	72.40	67.50	72.40	67.50	823	2498	0.826	7.6
syn.	X/✓	70.90	65.30	70.90	65.30	809	2509	0.823	7.6
def.	X	72.90	67.70	72.90	67.70	823	2489	0.826	4.3
	✓	72.10	67.10	72.10	67.10	812	2503	0.825	7.6

tracking rare or semantically similar classes becomes negligible, and the evaluation is dominated by the performance of dominant classes.

Inadequate Benchmarking. The prevalent strategies in MOT evaluation group tracking results based on class labels and evaluate each class separately. However, in large-scale datasets with inaccurate classification, this approach leads to inadequate benchmarking. Trackers that perform well in terms of localization and association but have inaccurate class predictions may receive low scores, even though their tracking results are valuable. For example, the trajectories of wrongly classified or unknown objects can still be useful for tasks such as collision avoidance in autonomous vehicles.

Table 8 presents our findings which indicate that the performance of the Grounded MOT system is very poor on the traditional benchmarking metrics (0.17% to 0.45% MOTA and -45.60% to -62.10% IDF1 on TAO). The benchmarking metrics for this task should be designed to differentiate between the two tasks of classification and tracking. By separating these tasks, the CA-MOTA and CA-IDF1 can help to provide a more accurate assessment of tracking performance.